

3D Subsurface Temperature Model of Germany and Upper Austria

Dr. Thorsten Agemar

Leibniz Institute for Applied Geophysics

11.07.2022

Introduction

Knowledge of the subsurface temperature is crucial for planning geothermal facilities. Higher temperatures give better energy yields and increase the cost-effectiveness of a geothermal site. In addition, project developers have to consider minimum temperatures due to technical constraints.

Mapping subsurface temperature distribution from available measurements is highly relevant for geothermal reservoir evaluations. Former investigations produced maps at certain depths with 2D-mapping algorithms (Schulz et al., 1992; Hurter and Schellschmidt, 2003). Besides the limited number of maps, the major disadvantage of 2D-algorithms is the loss of information from shallower levels. Furthermore, it is difficult to tackle inconsistent vertical temperature steps at specific locations.

Data

For the geothermal information system [GeotIS](#) (Agemar et al. 2014, Agemar et al. 2018), LIAG calculated a geostatistical temperature model of the subsurface based on the current data in the geophysics information system [FIS-Geophysik](#) (as of 28.09.2021) and a map of soil temperature covering Germany and Upper Austria. The resolution of the soil temperature data was reduced to a 4 km x 4 km grid. A detailed description of the soil temperature map was reported in Agemar et al (2012).

The subsurface temperature T in low enthalpy regions increases with depth d more or less linearly:

$$T = grad \cdot d + T_0 \quad (1)$$

For the model area, the geothermal gradient $grad$ varies by region but is typically in the range 25 to 100 K/km, with an average of about 30 K/km. T_0 is the average soil temperature which - except in the mountains - is in the range 7 to 11 °C. Regarding the temperature field down to 5 km below sea level, a conductive heat flow regime prevails in most regions. Here, the heterogeneity of the subsurface and the associated non-uniform thermal conductivity strongly affects the temperature distribution. However, in some areas, this conductive regime is superimposed by convective heat transport (e. g. Upper Rhine Graben).

The LIAG archives subsurface temperature data in the [FIS-Geophysik](#) for more than 20 years (Kühne et al. 2003). There exists a long tradition of measuring, collecting and evaluating subsurface temperature data at the LIAG (e. g. Schulz & Werner 1989, Schulz & Schellschmidt 1991, Schulz et al. 1992, Hurter & Schellschmidt 2003, Zschocke 2005, Agemar et al. 2012, Schumacher & Moeck 2020). [FIS-Geophysik](#) contains temperature data records 12.748. The data show a wide range of different qualities. Equilibrium temperature

logs can be regarded as high quality data that require no corrections. Periodic monitoring of production wells over many years provide reservoir temperatures that are also of high quality. Temperature measurements in the course of hydraulic production tests are generally also very good. The quality depends on the test duration. However, measurement results may be falsified by prior injection of cold water. Unfortunately, the bulk of subsurface temperature data is of lower quality. Bottom-hole temperatures (BHT), which are recorded in almost all industrial boreholes at the deepest point of a well or well section need to be corrected. Since BHTs are recorded immediately after drilling has stopped, the temperature field around the borehole is usually disturbed by mud circulation related to the drilling process. A number of methods to extrapolate from BHT to the undisturbed temperature have therefore been developed based on various assumptions about the cooling effect of the circulating mud and the thermal behaviour of the borehole and the surrounding rock (Hermanrud et al. 1990 and references therein, Goutorbe et al. 2007). Currently, four correction schemes for BHTs are in operation inside the [FIS-Geophysik](#) at the LIAG:

1. **Cylinder source model – CSM:** If three or more BHT values are available for one depth at different times after mud circulation stops, the thermal stabilization method for a cylindrical borehole can be used (Leblanc et al., 1982; Middleton, 1982). In this approach, the temperature of the mud when circulation stops ($t = 0$) is assumed to be constant, and varies by ΔT from the undisturbed rock temperature T_∞ :

$$T_\infty = T_{raw}(t) - \Delta T \left(e^{\frac{-a^2}{4\kappa t}} - 1 \right) \quad (2)$$

where	T_∞	= undisturbed rock temperature	[°C]
	T_{raw}	= measured bottom hole temperature	[°C]
	ΔT	= initial temperature disturbance	[K]
	a	= borehole radius	[m]
	κ	= thermal diffusivity	[m ² /s]
	t	= time after circulation stops (shut-in time)	[s]

The T_∞ is calculated by a fitting method varying ΔT and κ , where κ is the effective thermal diffusivity of the mud and the surrounding rock (Schulz et al., 1992). If the correlation coefficient of the linear regression is < 0.99 or deviates from CLSM correction by $\geq 5\%$, CLSM is used instead. The shortest shut-in times are discarded step by step if correlation coefficient is < 0.99 .

2. **Continuous line source model – CLSM:** If only two BHT values are available, a line source approach is derived from the negative heat transfer during the circulation time of the mud (Horner, 1951):

$$T_\infty = T_{raw}(t) - \frac{q}{4\pi\lambda} \ln \left(\frac{t+s}{t} \right) \quad (3)$$

where	q	= heat flow rate per length unit	[W/m]
	λ	= thermal conductivity	[W/mK]
	s	= circulation time	[s]

If circulation time s is unknown, it is set to 8 hours. CLSM is used if it yields a higher temperature than ILSM (see below).

3. **Instantaneous line source model – ILSM:** If only two BHT values are available and the circulation time can be ignored, a line source approach with an “explosion” heat sink is used (Lachenbruch and Brewer, 1959):

$$T_{\infty} = T_{raw}(t) - \frac{Q}{4\pi\lambda t} \quad (4)$$

where Q = heat per length unit [J/m]

ILSM is used when it yields a higher temperature than CLSM.

4. **Cylinder source model – CSM with lacking parameters:** If only one BHT value is available, the cylinder source model is used again. The initial temperature disturbance has to be estimated empirically. It correlates linearly with the difference between true formation temperature T_{∞} and raw temperature T_{raw} and reciprocally with borehole radius a (Agemar et al. 2022):

$$\Delta T = \frac{(T_{\infty} - T_0)}{31a} \quad (5)$$

With this correlation, formula (2) can be transformed to:

$$T_{\infty} = \frac{T_{raw}(t) \cdot 31a + T_0 \left(e^{\frac{-a^2}{4\kappa t}} - 1 \right)}{31a + \left(e^{\frac{-a^2}{4\kappa t}} - 1 \right)} \quad (6)$$

If the shut-in time is unknown, it is estimated on the basis of another empirical correlation. As described by Bolotovskiy et al. (2015), the shut-in time t [s] is determined as a function of the measurement depth z [m]:

$$t = 3600 \cdot (3.612 + 0.001639 \cdot z) \quad (7)$$

Formula (7) is the result of linear regression based on mean shut-in times for specific depth intervals and a maximum shut-in time of 24 hours.

For the CSM corrections, a fixed thermal diffusivity κ of $0.15 \cdot 10^{-6}$ [m²/s] was chosen which was determined on the basis of experience, numerical tests and statistical data (Schulz and Werner 1987). The value is close to the value for pure water. Obviously, the thermal diffusivity of the drilling fluid is very relevant because rocks have a much higher thermal diffusivity. The temperature sensitivity of the thermal diffusivity of water is neglected.

The estimation of temperature data uncertainty is based on previous studies at the LIAG (Schulz et al 1992, Agemar et al. 2012, Agemar 2022). Comparisons of different data qualities is the key to good uncertainty estimation. However, the uncertainty does not only depend on the measurement and correction method. A large correction inevitably implies a larger uncertainty. Generally, lower formation temperatures show less uncertainty because mud circulation had less influence. The difference between true formation temperature T_{∞} and raw temperature T_{raw} is crucial. Table 1 gives details on the estimation of input data uncertainty.

Tab. 1: Uncertainty estimate of corrected BHTs and other temperature records. The term $(T_{\infty} - T_{raw})$ represents the smallest difference between undisturbed formation temperature and measured temperature. The variable d_{max} refers to the total depths.

Temperature data type	Estimation of standard deviation [°C]
BHT single measurement, shut-in time unknown CSM correction	$0,96 \cdot (T_{\infty} - T_{raw})$, minimum: 3,0
BHT with 1 shut-in time CSM correction	$0,87 \cdot (T_{\infty} - T_{raw})$, minimum: 3,0
BHT with 2 shut-in times CLSM correction	$0,75 \cdot (T_{\infty} - T_{raw})$, minimum: 3,0
BHT with 2 shut-in times ILSM correction (circulation time ignored)	$0,75 \cdot (T_{\infty} - T_{raw})$, minimum: 3,0
BHT with more than 2 shut-in times CSM correction	$0,70 \cdot (T_{\infty} - T_{raw})$ minimum: 3,0
Non-equilibrium temperature log	$0,2 \cdot \sqrt{d_{max}}$
Temperature recording during hydraulic testing	2,5
Undisturbed reservoir temperatures from long time monitoring, equilibrium temperature logs, mining temperatures	0,01

Individual points were interpolated linearly in 100 m steps along vertical, virtual well paths. This step is required for better 3d kriging estimates. The soil temperature was used for the depth $d = 0$ m. Based on experience, the standard deviation σ of these virtual logs was estimated with a root function according to:

$$\sigma(d) = \sigma(d_{max}) \sqrt{\frac{d}{d_{max}}} \quad (8)$$

$$\begin{aligned} \text{where } d &= \text{depth} & [\text{m}] \\ d_{max} &= \text{depth of the measurement} & [\text{m}] \end{aligned}$$

Method

The geostatistical calculation was carried out using the ISATIS.NEO® software (V2021.12.1) from Geovariance. The result was exported to Gocad/SKUA® software by Emerson and saved as a Voxet file. The previous temperature models of the subsurface were calculated with Gocad/SKUA® in 2018. The advantage of ISATIS.NEO is that this geostatistical software takes into account the different qualities of the input data. This eliminates filtering steps in the workflow. In previous temperature models, low-quality measurements in spatial proximity to good measurements were removed from the input dataset. While three quality categories were used for the first temperature models for [GeotIS](#), four categories were used in 2018. In the current model, the input dataset was not filtered. Only for measurements less than 100 m apart a filter was applied. With this new approach much less data is discarded.

The 3d temperature model has been calculated using the universal kriging method, also known as kriging with trend. Here, the geothermal gradient is removed from the measured values before calculation and then added again. Thus, kriging is carried out with the residual temperature in the unit °C. A normal score transformation was not applied to the input data in order to maintain linear interpolation. However, this has implications for the kriging result, as the input data only roughly follow the Gaussian normal distribution. There exists a slight

positive skew in the data. Thus, the uncertainty given as kriging standard deviation is not really symmetric.

ISATIS allows the search ellipsoid to be divided into sectors to stabilise the kriging calculation. Since the data density decreases with depth, the search ellipsoid (radius 300 km, vertical extent 3 km) was halved horizontally and 800 data points for each half were targeted. This is relevant for balancing the amount of used data above or below the estimated grid node.

The criteria of stationarity are not fulfilled over the whole area of Germany. Some areas, like for instance the Upper Rhine Graben area show very high spatial variability due to upwelling of deep thermal water. This also has implications for any attempt to extrapolate to deep subsurface because many depth-temperature profiles in the Upper Rhine Graben are far from linear (Agemar et al 2012, Schulz & Schellschmidt 1991, Clauser & Villinger 1990).

Therefore, the model area has been split into three parts: Northern Germany, South Western Germany (mainly Upper Rhine Graben area) and South Eastern Germany plus Upper Austria. For each part, an individual semi-variogramme has been estimated and kriging carried out. Fig. 1 shows the horizontal semi-variogramme models which have been fitted to the data.

A crucial aspect of 3d kriging is the balancing of horizontal and vertical range. While the horizontal range is well constrained, estimates of the vertical range rely on very few temperature logs and the vertical semi-variogrammes hardly show a plateau (sill). To achieve an optimal weighting of spatially distributed measurements, the sill for horizontal and vertical semi-variogrammes should be approximately the same. Kriging parameters derived from spatial variability analyses are listed in Tab. 2. Note that vertical range for SW-Germany is much lower than for the other model areas.

The three 3d subsurface temperature models have been merged together using the 3d modelling software Gocad/SKUA®. Finally, the same software was also used to check consistency and to remove isolated negative gradients (temperature decrease with depth) by raising the temperature to the level of the grid node above. Such negative gradients are unlikely in the deep subsurface of Germany because there exists no high enthalpy geothermal field. Negative gradients are interpolation artefacts and occur when deep wells with low gradients are located near shallow wells with high gradients. They have never been measured in the deep subsurface of Germany.

Tab. 2: Kriging parameters derived from semi-variogrammes for three regions.

	SW-Germany	SE-Germany + Upper Austria	N-Germany
Nugget	30 K ²	4 K ²	1 K ²
Sill	410 K ²	135 K ²	70 K ²
Range horizontal	30 km	70 km	90 km
Range vertical	1000 m	2000 m	2000 m
Type	Spherical	Spherical	Spherical

Result

The 3d subsurface temperature model is available as orthogonal grids with 2 km spacing in W-E and S-N direction on Gauß-Krüger coordinates (9° central meridian). Vertically, layers are produced in 100-m-steps from 5000 m below sea level. Temperature and kriging standard deviation are given in °C. The public geothermal information system [GeotIS](#) uses this temperature model for visualising the subsurface temperature field on interactive cross

sections, horizontal cuts and stratigraphic horizons since 7th of June 2022. Fig. 2 is a screenshot from [GeotIS](#) and shows the lateral extend of the 3d subsurface temperature model. The 3d subsurface temperature model basically covers Germany and Upper Austria. However, temperatures in areas of no data are flagged with no-data-values.

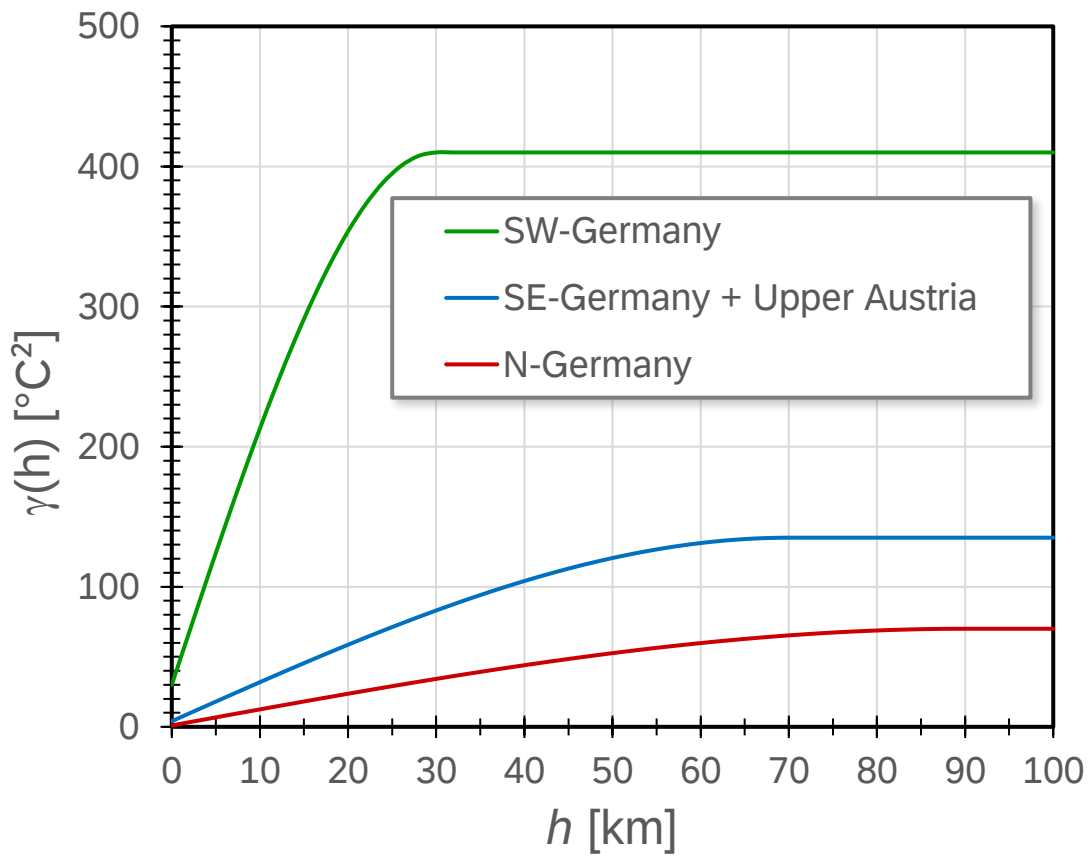


Fig 1. Semi-variogramme models (spherical) for different areas: South Western Germany, South Eastern Germany + Upper Austria and Northern Germany.



Fig. 2: Extend of 3d temperature model

Discussion

The 3d model represents the best interregional temperature estimate of the subsurface in Germany and Upper Austria. The method universal kriging offers the best unbiased, linear approximation based on measured data. It also offers uncertainty estimates as kriging standard deviation which is important to assess the risk of not reaching a target temperature at a specified depth.

The 3d subsurface temperature model benefits from using modern geostatistics software. The possibility to use kriging weights has been introduced by Delhomme (1978). The current estimates of measurement uncertainty and its extension on vertically interpolated virtual logs are based on experience and statistical approximations. They might be subject to changes in future 3d subsurface temperature models when more data become available.

In order to take into account the varying degrees of spatial variability, three submodels have been calculated and merged. However, the spatial variability also changes with depth. The highest spatial variability is normally found at 2 to 3 km depth (Agemar et al. 2012). A segmentation into different depth regions has not been realised so far. This offers potential for improvement for future temperature models. The current method tends to overestimate uncertainty in the shallow subsurface.

Terms of use

The 3d subsurface temperature model is provided by the LIAG under specific terms and conditions. The LIAG assumes no responsibility for the correctness, completeness, quality or usability of this model. It can be used for commercial and non-commercial purposes. It is only permitted to reproduce and share the original model or any derived work in part not covering more than four federal states (Bundesländer). In case of any distribution or publishing it is mandatory to name the original creator and the LIAG, keep the copyright notice and disclaimer intact and visible.

References

- Agemar, T. (2022) Bottom hole temperature correction based on empirical correlation. – *Geothermics* 99. 7p. doi.org/10.1016/j.geothermics.2021.102296
- Agemar, T., Alten, J.-A., Ganz, B., Kuder, J., Kühne, K., Schumacher, S., Schulz, R. (2014) The Geothermal Information System for Germany – GeotIS. – *Z. Dt. Ges. Geowiss.*, 165(2): 129-144.
- Agemar, T., Schellschmidt, R., Schulz, R. (2012) Subsurface Temperature Distribution of Germany. – *Geothermics* 44: 65– 77. doi: 10.1016/j.geothermics.2012.07.002
- Agemar, T., Weber, J., Moeck, I. S. (2018) Assessment and Public Reporting of Geothermal Resources in Germany: Review and Outlook. *Energies* 11(2): 332. doi: 0.3390/en11020332
- Bolotovskiy, I., Schellschmidt, R., Schulz, R. (2015) Fachinformationssystem Geophysik: Temperaturkorrekturverfahren. LIAG-Bericht, Archiv-Nr. 0132527; Hannover.
- Delhomme, J.P., 1978. Kriging in the hydrosiences. *Advances in Water Resources* 1 (5), 251–266. doi.org/10.1016/0309-1708(78)90039-8
- Dose, T., 2006. Geostatistical estimation of temperatures – an example from the Upper Rhine Graben. In: DGMK – Frühjahrstagung 2006. Celle, Germany, pp. 533–545.
- Goutorbe, B., Lucazeau, F., Bonneville, A. (2007) Comparison of several BHT correction methods: a case study on an Australian data set. *Geophys. J. Int.* 170, 913-922. doi: 10.1111/j.1365-246X.2007.03403.x

- Hermanrud, C., Cao, S., Lerche, I., (1990) Estimates of virgin rock temperature derived from BHT measurements: Bias and error. *Geophysics* 55(7), 924-931.
- Hurter, S., Schellschmidt, R., 2003. Atlas of geothermal resources in Europe. –*Geothermics* 32, 779–787.
- Kühne, K., Maul, A.-A., Gorling, L. (2003) Aufbau eines Fachinformationssystems Geophysik. – *Z. Angew. Geol.* 2/2003: 48-53; Hannover.
- Leblanc, Y., Lam, H.-L., Pascoe, L.J., Johnes, F.W. (1982) A comparison of two methods of estimating static formation temperature from well logs. –*Geophys. Prosp.*, 30: 348-357.
- Middleton, M.F. (1982) Bottom-hole temperature stabilization with continued circulation of drilling mud. – *Geophysics*, 47: 1716-1723.
- Schulz, R., Hänel, R., Kockel, F. (1992) Federal Republic of Germany - West federal states. - In: Hurtig, E., Cermak, V., Haenel, R. & Zui, V. (Eds.): *Geothermal Atlas of Europe*: 34-37; Gotha.
- Schulz, R., Schellschmidt, R. (1991) Das Temperaturfeld im südlichen Oberrheingraben. – *Geol. Jb.*, E48: 153-165; Hannover.
- Schulz, R., Werner, K.H. (1987) Einfache Korrekturverfahren für Temperaturmessungen. – *NLFB-GGA-Bericht*, Archiv-Nr. 99914; Hannover.
- Schulz, R., Werner, K.H., 1989. Geothermal resources and reserves: updating of temperature data base. In: Louwrier, K., Staroste, E., Garnish, J., Karkoulas, D. (Eds.), *European Geothermal Update: Proceedings of the 4th International Seminar on Results of EC Geothermal Energy Research and Demonstration*. Kluwer Academic Publishers, Dordrecht, pp. 490–499.
- Schumacher, S., Moeck, I. (2020) A new method for correcting temperature log profiles in low-enthalpy plays. *Geotherm Energy* 8, 27 (2020). doi: 10.1186/s40517-020-00181-w
- Zschocke, A. (2005) Correction of non-equilibrated temperature logs and implications for geothermal investigations. –*J. Geophys. Eng.* 2 (2005) 364–371.

WEB-LINKS

FIS-GP: <https://www.fis-geophysik.de> Leibniz Institute for Applied Geophysics, Hannover.
 GeotIS: <https://www.geotis.de> Leibniz Institute for Applied Geophysics, Hannover.